Problems associated with having the gap on the boundary can be avoided by raising the FEM/MoM boundary above the gap, effectively increasing the size of the FEM region. Then, small tetrahedral elements can be used around the gap and a coarse triangular mesh can be used on the MoM boundary. Computational resources are reduced using this approach because the increased memory requirements to model the FEM region are more than offset by the reduction in memory required to model the MoM surface. Numerical results obtained using this approach agree well with measurements.

REFERENCES

[1] T. F. Eibert and V. Hansen, "3-D FEM/BEM-hybrid modeling of surface mounted devices within planar circuits," *IEEE Trans. Microwave Theory Tech.*, vol. 46, pp. 1334–1336, Sept. 1998.

[2] Y. Ji and T. H. Hubing, "EMAP5: A 3D hybrid FEM/MoM code," *Appl. Computat. Electromagn. Soc. (ACES) J.*, vol. 15, pp. 1–12, 2000.

[3] H. Wang, Y. Ji, T. H. Hubing, and J. L. Drewniak, "Radiation from right angle bends in microstrip traces," in *Proc. IEEE Int. Symp. Electromag. Compat.*, Washington, DC, Aug. 2000.

[4] "Pentium III Processor Power Distribution Guidelines," Intel Corp., Intel App. Note AP-907, order 245 085-001, 1999.

[5] Z. Soe, "Layout Guideline for the RC7100 Motherboard System Clock," Fairchild Semiconductor Corporation, Fairchild Semiconductor App. Bull. AB-19, stock no. AB00 000 019, 1998.

[6] J. Chen *et al.*, "Power-bus isolation using power islands in printed circuit boards," *IEEE Trans. Electromagn. Compat.*, vol. 44, pp. 373–380, May 2002.

[7] A. F. Peterson, S. L. Ray, and R. Mittra, *Computational Methods for Electromagnetics*. New York: IEEE Press, 1997, ch. 11.

[8] M. L. Barton and Z. J. Cendes, "New vector finite elements for three-dimensional magnetic field computation," *J. Appl. Phys.*, vol. 61, pp. 3919–3921, 1987.

[9] J. L. Volakis, A. Chatterjee, and L. C. Kempel, *Finite Element Method for Electromagnetics*. New York: IEEE Press, 1998, pp. 56–59.

[10] S. M. Rao, D. R. Wilton, and A. W. Glisson, "Electromagnetic scattering by surfaces of arbitrary shape," *IEEE Trans. Antennas Propagat.*, vol. AP-30, pp. 409–418, May 1982.

[11] J. J. H. Wang, *Generalized Moment Methods in Electromagnetics*. New York: Wiley, 1990.

[12] Y. Ji, H. Wang, and T. H. Hubing, "A novel preconditioning technique and comparison of three formulations for the hybrid FEM/MoM method," *Appl. Computat. Electromagn. Soc. (ACES) J.*, vol. 15, pp. 103–114, 2000.

[13] Y. Ji and T. H. Hubing, "On the interior resonance problem when applying a hybrid FEM/MoM approach to model printed circuit boards," *IEEE Trans. Electromag. Compat.*, vol. 44, pp. 318–323, May 2002.

[14] C. Wang, "Determining Dielectric Constant and Loss Tangent in FR-4," Electromagnetic Compatibility Lab., Dep. Elect. Comput. Eng., University of Missouri-Rolla, Rolla, MO, TR00-1-41.

[15] J. Van Bladel, *Singular Electromagnetic Fields and Sources*. New York: Oxford Univ. Press, 1991, ch. 4.

Finite-Element Modeling of Coaxial Cable Feeds and Vias in Power-Bus Structures

Hao Wang, Yun Ji, and Todd H. Hubing

***Abstract*—This paper presents three different models that can be used to represent coaxial cable feeds or vias in printed circuit board power-bus structures. The *probe model* represents a coaxial feed or via as a current filament with unknown radius. The *coaxial-cable model* enforces an analytical field distribution at the cable opening or via clearance hole. The *strip model* employs the equivalent radius concept to represent cylindrical feeds and vias as rectangular strips. Although the strip model is functionally equivalent to two closely positioned probe models, it accurately represents the conductor radius and is more accurate in situations where the via or feed radius is important.**

***Index Terms*—Circuit board modeling, edge elements, finite-element method (FEM), method of moments (MOM).**

I. INTRODUCTION

Multilayer printed circuit boards (PCBs) and multichip modules (MCMs) often employ a power-bus structure consisting of solid power-return plane pairs. At low frequencies, the behavior of the power-bus structure can be modeled using lumped elements [1]. At frequencies where the dimensions of the board are not electrically small, it is necessary to use complex distributed models. In the frequency domain, two numerical methods often used to analyze PCB structures are the method of moments (MoM) and the finite-element method (FEM).

It is critical to accurately represent sources and vias when modeling the behavior of PCB power-bus structures. When making measurements, these structures are often driven with a coaxial cable. The outer conductor of the coaxial cable is connected to the reference plane and the center conductor extends through to the power plane. The reference plane is normally calibrated to the cable opening, where the center conductor begins to extend beyond the outer conductor. The term via commonly refers to a plated-thru hole in a PCB. A via can be used for mounting a through-hole component or for routing signals between layers. The geometry of vias and coaxial feeds is similar. Both consist of an opening in one or both planes and a vertical conductor that may or may not connect to each plane.

This paper investigates three models that can be used to represent sources and vias in a PCB power bus. The *probe model* represents coaxial cable feeds and vias using one finite-element or moment-method-element edge. The *coaxial-cable model* enforces the analytical field distribution at the opening in the reference plane and includes the effects of the finite radius of the vertical conductor. The *strip model* employs the equivalent radius concept [2] to replace cylindrical feeds or vias with rectangular strips. These three models have been implemented in a hybrid FEM/MoM code. Two practical power-bus structures are investigated to validate and compare the three models.

Manuscript received March 15, 2002; revised June 19, 2002.

H. Wang and T. H. Hubing are with the Department of Electrical and Computer Engineering, University of Missouri-Rolla, Rolla, MO 65409 USA.

Y. Ji is with the Desktop Architecture Laboratory, Intel Corporation, Hillsboro, OR 97124 USA

Digital Object Identifier 10.1109/TEMC.2002.804776

0018-9375/02$17.00 © 2002 IEEE

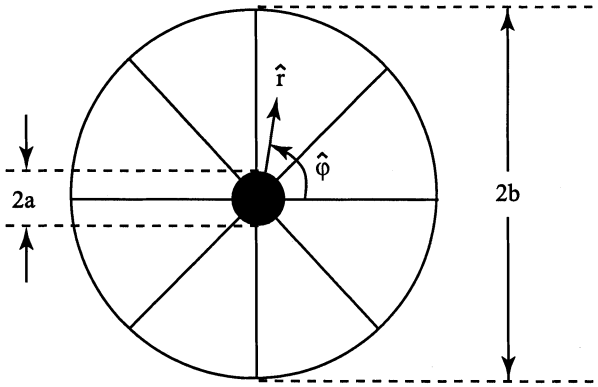

Fig. 1. Cross section of a coaxial cable feed.

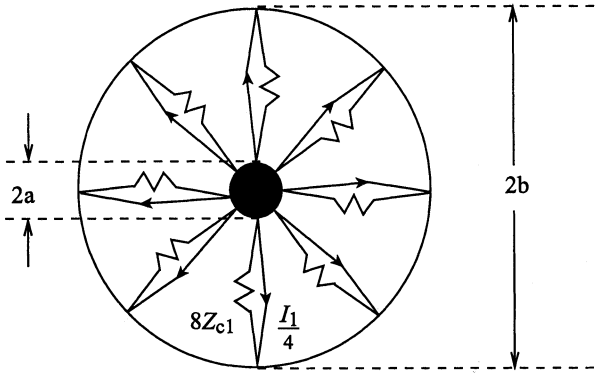

Fig. 2. A simplified coaxial cable model ($N = 8$).

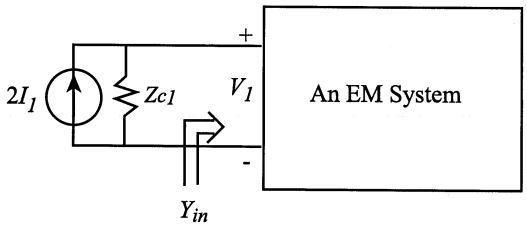

Fig. 3. Block diagram of a system excited using the coaxial-cable model.

II. The Probe Model

Fig. 1 illustrates the cross section of a coaxial cable feed, which has a center conductor, an outer conductor, and a dielectric between the two conductors. The probe model uses an impressed electric current to model the source [3], [4]. The center conductor is represented by an infinitesimally thin current filament that extends between the power and ground planes. The opening in the plane is replaced with a perfect electric conductor (PEC). The PEC boundary condition along the center conductor cannot be enforced, otherwise the power and ground plane would be shorted.

The weak form of the vector Helmholtz equation is shown in (1) at the bottom of the page. A source term $[g^{\text{int}}]$ representing sources located within the FEM region is given by

$$\mathbf{g}^{\text{int}} = -\int_{V_2}\left[\mathbf{J}^{\text{int}}(\mathbf{r}) + \frac{1}{j\omega\mu_0\mu_r}\nabla\times\mathbf{M}^{\text{int}}(\mathbf{r})\right]\bullet\mathbf{w}(\mathbf{r})dV \quad (2)$$

where $\mathbf{w}(\mathbf{r})$ is the set of volume basis functions.

An impressed current source in z-direction can be expressed as

$$\mathbf{J}^{\text{int}} = I_1\delta(x-x_f)\,\delta(y-y_f)\,\hat{\mathbf{z}} \quad (3)$$

where (x_f, y_f) specifies its position, I_1 denotes the electric current magnitude and $\delta(x)$ is the Dirac delta function. The contribution to vector $\boldsymbol{g}^{\text{int}}$ in (2) is then simply

$$\mathbf{g}^{\text{int}} = I_1\int\int\int \hat{z}\bullet\{\mathbf{w}\}\delta(x-x_f)\,\delta(y-y_f)\,dxdydz. \quad (4)$$

If the basis functions $\mathbf{w}_m(\mathbf{r})$ are Whitney elements [5], the source term in the FEM equation is given by

$$\left[g^{\text{int}}\right]^e = I_1 l_1 \quad (5)$$

where l_1 is the edge length. The input impedance can be calculated as follows:

$$Z_{in} = \frac{V_1}{I_1} = \frac{E_1 l_1}{I_1} \quad (6)$$

where E_1 is the electric field along the source edge.

It is a common practice to model the source using one edge. However, it is possible to model the source using several edges in series. In such a case, the source voltage is the sum of the voltages on the source edges. Vias can be modeled in a similar manner without enforcing a source current. Commonly, vias are modeled simply by forcing the electric field on a single vertical edge to be zero. The probe model is widely used and is capable of generating satisfactory results for thin, electrically short feeding structures [4].

III. The Coaxial-Cable Model

In some applications, the probe model is too simplistic and a more detailed representation of the source is required. A coaxial-cable model for FEM proposed by Gong and Volakis [6] assumes a TEM field distribution in the cable opening

$$\mathbf{E} = \frac{e_0}{r}\hat{\boldsymbol{r}} \quad (7)$$

$$\mathbf{H} = \frac{h_0}{r}\hat{\phi} \quad (8)$$

where e_0 and h_0 are parameters satisfying

$$e_0 = \frac{I_1 Z_{c1}}{2\pi\sqrt{\varepsilon_{rc}}}(1+\Gamma) \quad (9)$$

$$h_0 = \frac{I_1}{2\pi}(1-\Gamma) \quad (10)$$

$$h_0 = -\frac{\sqrt{\varepsilon_{rc}}}{Z_{c1}}e_0 + \frac{I_1}{\pi} \quad (11)$$

$$\int_{V_2}\left[j?\varepsilon_0\varepsilon_r\mathbf{E}(\mathbf{r})\bullet\mathbf{w}(\mathbf{r}) + \frac{(\nabla\times\mathbf{E}(\mathbf{r}))\bullet(\nabla\times\mathbf{w}(\mathbf{r}))}{j?\mu_0\mu_r}\right]dV$$
$$= \int_{S_2}(\hat{n}\times\mathbf{H}(\mathbf{r}))\bullet\mathbf{w}(\mathbf{r})dS - \int_{V_2}\left[\mathbf{J}^{\text{int}}(\mathbf{r}) + \frac{1}{j\omega\mu_0\mu_r}\nabla\times\mathbf{M}^{\text{int}}(\mathbf{r})\right]\bullet\mathbf{w}(\mathbf{r})dV \quad (1)$$

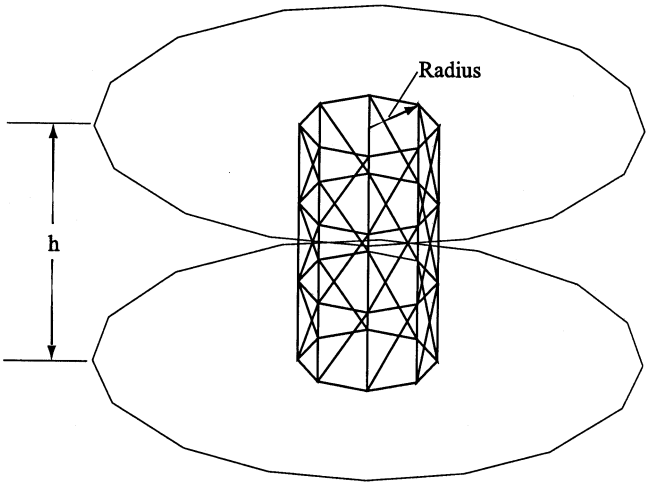

Fig. 4. The mesh for the center conductor of a coaxial-cable feed or a via.

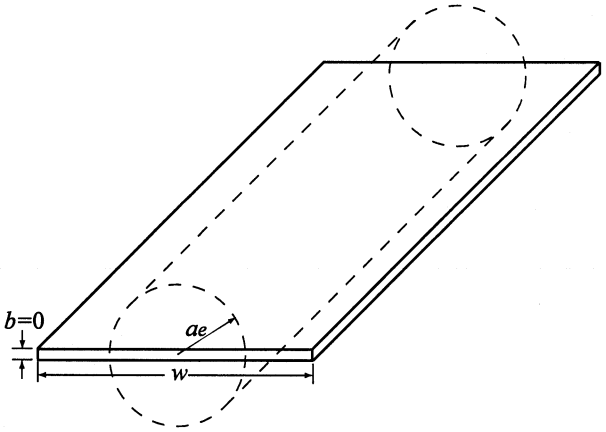

Fig. 5. Electrical equivalent radius.

where I_1 is the *incident* current in the cable, ε_{rc} is the relative permittivity of the dielectric inside the cable, Γ is the reflection coefficient and Z_{c1} is the characteristic impedance of the cable. The equipotential condition is enforced at the cable opening as follows:

$$\begin{aligned}\Delta V =& E_i(b-a) = e_0 \ln\left(\frac{b}{a}\right)\\ E_i \in& \{\text{unknowns at the cable junction, } i = 1,\ldots,N\}\end{aligned} \tag{12}$$

where a and b are the radii of the center and outer conductors and N is the total number of unknowns on the cable interface. In [6], the cable excitation was derived from an FEM formulation based on the variational method, which is equivalent to an FEM formulation based on the weak form and Galerkin's method. Analytical evaluation of the field in the cable opening [first term on the right-hand side of (1)] is given by [6]

$$f_i^c = \int_{S_c} (\hat{n} \times \mathbf{H}(\mathbf{r})) \bullet \mathbf{E}(\mathbf{r}) dS = C_i E_i - f_i \tag{13}$$

where

$$C_i = \frac{2\pi\sqrt{\varepsilon_{rc}}(b-a)^2}{N \ln\left(\frac{b}{a}\right)\eta_0} \tag{14}$$

$$f_i = \frac{2(b-a)I_1}{N}. \tag{15}$$

C_i is added to the diagonal entries corresponding to the cable edges in the FEM matrix and f_i^c is added to the FEM source entries corresponding to the cable edges. After E_i is determined, the input admittance is given by

$$Y_{in} = \frac{2I_1}{V_1} - \frac{1}{Z_{c1}} \tag{16}$$

where V_1 is the voltage along the cable edges. In the coaxial-cable model, the PEC boundary condition along the center conductor is strictly enforced. The dielectric opening at the coaxial cable is modeled using FEM.

Fig. 2 illustrates a relatively simple coaxial-cable model with $N = 8$ elements representing the field in the opening. The elements are connected in parallel therefore the total impedance is Z_{c1}. The current sources are also connected in parallel so the total current flowing from the center conductor to the outer conductor is $2I_1$. Fig. 3 shows a block diagram of an electromagnetic system excited by a coaxial cable model. Y_{in} satisfies the relationship in (16). Fig. 4 illustrates a triangular mesh for the center conductor of the coaxial cable model in Fig. 2. This triangular mesh also can be used to model a via. The PEC boundary condition is enforced on the via's cylindrical wall.

IV. The Strip Model

Although the coaxial-cable model can be used to represent coaxial cable feeds and vias accurately, it is relatively complicated to work with. Generating the mesh can be time consuming and the computational resources required can be excessive when the number of vias is large. A compromise between the complex coaxial-cable model and the simplistic probe model is achieved by using the concept of equivalent radius to represent cylindrical vias using flat elements. A thin rectangular strip of width, w, has an equivalent radius $a_e = 0.25w$ as illustrated in Fig. 5 [3]. Fig. 6 shows a mesh employed around the coaxial cable feed or via using the rectangular current strip. To model a coaxial feed, two current sources are located at the two sides of the rectangular strip and connected in parallel so that the total current flowing from the lower plane to the upper plane is $2I_1$. To model a via, the two sides of the rectangular strip are modeled as two PEC edges.

V. Numerical and Experimental Results

Two PCB power-bus geometries were investigated to validate and compare the three feed and via models. Fig. 7 shows the first geometry consisting of two copper planes representing the power and ground planes of a PCB. The board dimensions are 100 mm × 50 mm × 1.1 mm. The dielectric between the PEC layers has a relative permittivity of $4.7(1 - j0.02)$. A coaxial standard connector designator (SMA) connector feeds the structure at the locations (30 mm, 20 mm) indicated in Fig. 7. The radius of the center conductor of the SMA connector is 0.635 mm. An impedance analyzer was used to measure the input impedance at the cable opening. Numerical results were obtained using a hybrid FEM/MoM code. Fig. 8 shows the magnitude of the input impedance. It is evident that the measurements and the numerical results, obtained using the coaxial-cable model and the strip model, agree with the measurement very well from 100 to 600 MHz, while the probe model fails to generate satisfactory results. The input impedance null near 360 MHz is shifted 40 MHz (10%) to the left in the probe-model results. This null correspondences to the zero in the expression for the input impedance and can be calculated in a straight-forward manner using [1]

$$f_O = \frac{1}{2\pi\sqrt{LC_b}} \tag{17}$$

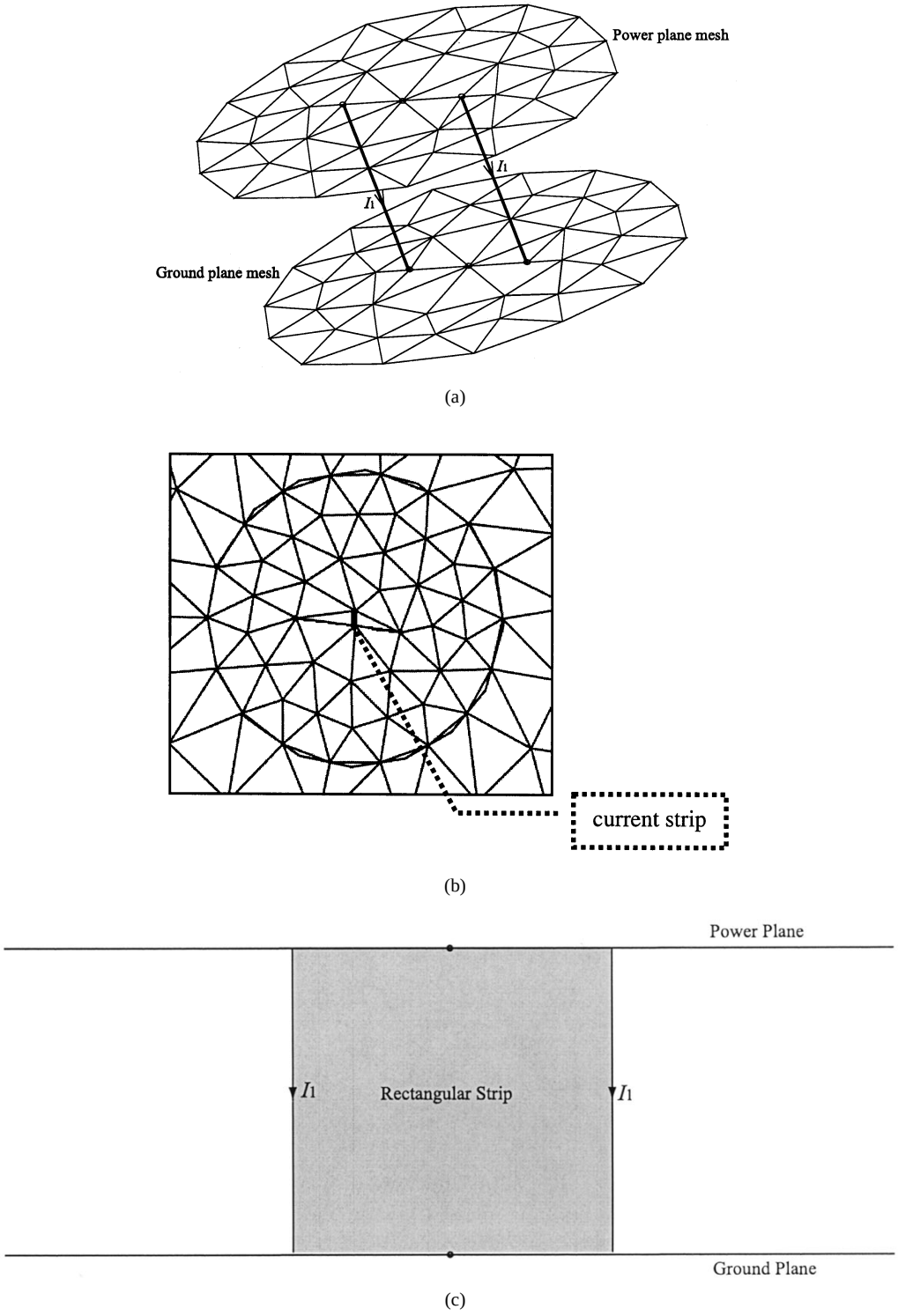

Fig. 6. The EMAP5 mesh around the current strip source or the via. (a) Three-dimensional view. (b) Top view. (c) Side view.

where C_b is the interplane capacitance and L is the "effective" inductance of the via [7], [8].

It is perhaps not surprising that the probe-model results are not accurate. The effective inductance of the SMA connector is a function of the conductor radius [7], [8]. The probe model does not have a well-defined conductor radius. Although the strip model has a well-defined radius, it is essentially just two probe models located very near each other.

Table I shows the number of tetrahedra and FEM unknowns used to model the cylindrical volume surrounding a via as shown in Fig. 6(a). Improved accuracy is obtained with less computer resources using the strip model.

In order to demonstrate that the improved accuracy of the strip model is not due to the slightly finer mesh density required to place two edges in close proximity, the strip model example was rerun using the same mesh, but with only one source edge (probe model). Fig. 9 illustrates the probe-model result that uses the strip model's fine mesh and compares it with other results. Despite using the same mesh, the strip model yields a more accurate result than the probe model. In fact, the strip

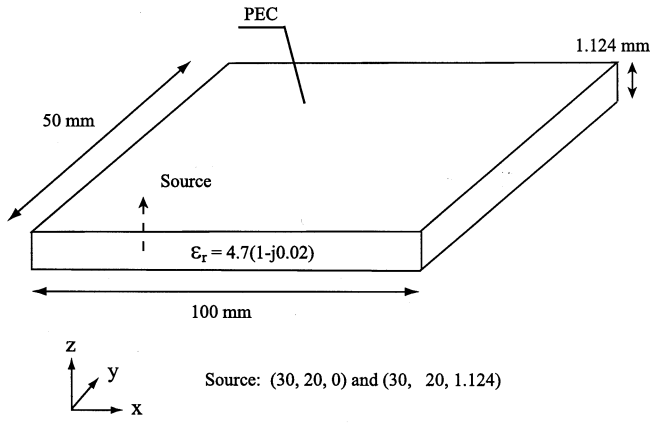

Fig. 7. Geometry of an open power-bus structure.

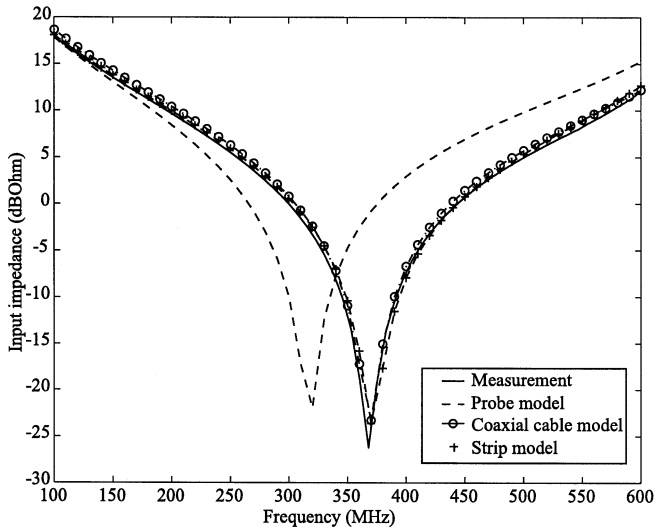

Fig. 8. Comparison between models and measurements for the open power-bus structure C_b.

TABLE I
COMPARISON BETWEEN DIFFERENT MODELS

	Probe model	Coaxial-cable model	Strip model
Tetrahedra numbers	104	372	188
FEM unknowns	175	623	312

model result is nearly identical to the much more complex coaxial-cable model result.

The second geometry investigated here is a shorted power-bus structure that has the same dimensions and feed location as the first power-bus structure as illustrated in Fig. 10. A via centered at (40 mm, 20 mm) connects the power and ground planes. The radius of the via is 0.254 mm. Fig. 11 compares the numerical and measured results. The probe model fails to generate satisfactory results while good agreement is achieved between the measurement and numerical results using the coaxial cable model or strip model. For the probe-model result, the left shift at the first peak (369 MHz) can be equated to excess inductance at the coaxial cable feed, while the left shift at the second peak (440 MHz) equates to excess inductance at the via [7]. The probe model does not accurately represent the via radius and therefore does not correctly determine the effective inductance of the via.

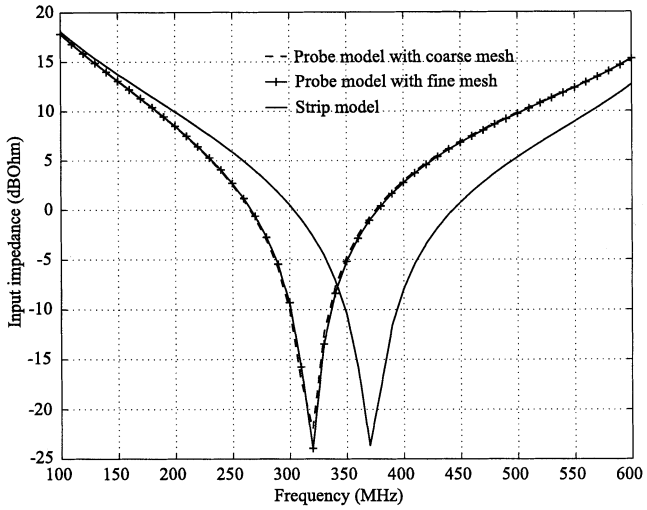

Fig. 9. Comparison between the probe-model and strip-model results.

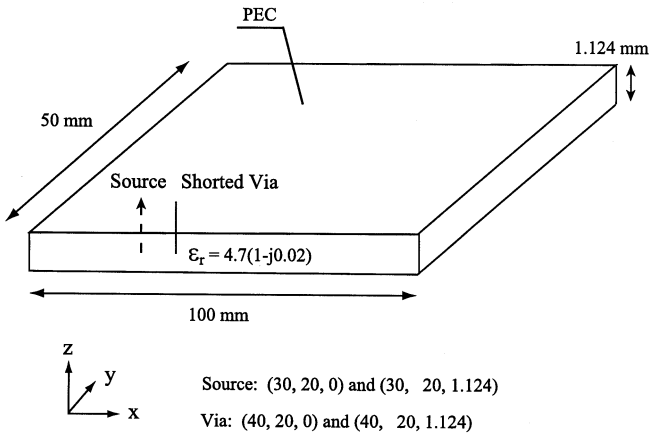

Fig. 10. Geometry of a shorted power-bus structure.

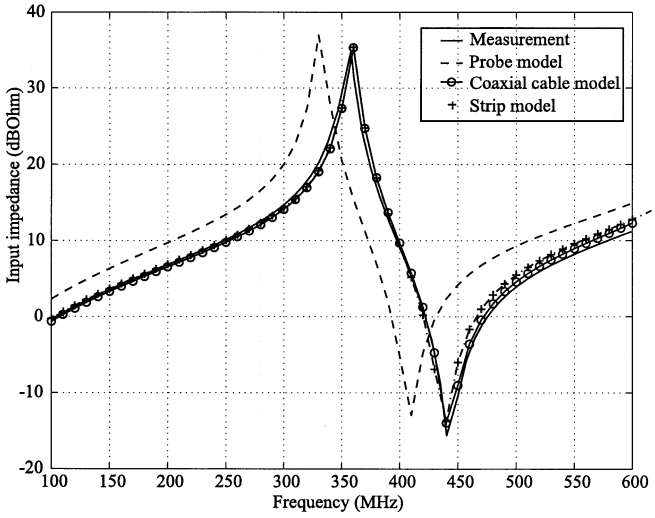

Fig. 11. Comparison between models and measurements for the shorted power-bus structure.

VI. Conclusions

Three different approaches for modeling coaxial cable feeds and vias in power-bus structures have been described. The probe model is easy to implement and is very effective for modeling thin, electrically short feeding structures. However, it cannot be used to accurately model configurations where the feed or via radius is an important parameter. The coaxial-cable model assumes a TEM field distribution at the cable opening. The field in the opening is analytically evaluated and the boundary conditions along the center conductor and at the cable opening are strictly enforced. Although the coaxial-cable model can represent the coaxial-cable source and vias accurately, it is relatively difficult to generate meshes for the center conductor and the clearance hole. When the number of the vias is large, the additional elements required by the coaxial-cable model can consume significant computer resources.

A relatively simple strip model employs the equivalent radius concept to simplify the mesh procedure by representing the feeds and the vias as rectangular strips. This model can be used at all frequencies where the structure being modeled is electrically small. The strip model is simpler to implement than the coaxial-cable model, but accurately represents coaxial feeds or vias with a finite radius.

References

[1] T. H. Hubing, J. L. Drewniak, T. P. Van Doren, and D. M. Hockanson, "Power bus decoupling on multiplayer printed circuit boards," *IEEE Trans. Electromagn. Compat.*, vol. 37, pp. 155–166, May 1995.

[2] C. A. Balanis, *Antenna Theory*, 2nd ed. New York: Wiley, 1997, pp. 454–457.

[3] D. M. Pozar, "Input impedance and mutual coupling of rectangular microstrip antenna," *IEEE Trans. Antennas Propagat.*, vol. 30, pp. 1191–1196, Nov. 1982.

[4] J. -M. Jin, *The Finite Element Method in Electromagnetics*. New York: Wiley, 1993, pp. 324–325.

[5] J. C. Nedelec, "Mixed finite elements in R3," *Num. Math.*, vol. 35, pp. 315–341, 1980.

[6] J. Gong and J. L. Volakis, "An efficient and accurate model of the coax cable feeding structure for FEM simulation," *IEEE Trans. Antennas Propagat.*, vol. 43, pp. 1474–1478, Dec. 1995.

[7] J. Fan, "Modeling and Design of DC Power Buses in High-Speed Digital Circuit Designs," Ph.D. dissertation, Dep. Elect. Comput.Eng., Univ. of Missouri-Rolla, Rolla, 2000.

[8] M. Xu, Y. Ji, T. H. Hubing, T. P. Van Doren, J. L. Drewniak, and R. E. DuBroff, "Development of a closed-form expression for the input impedance of power-ground plane structures," in *Proc. 2000 IEEE Int. Symp. Electromagnetic Compatibility*, Washington, DC, Aug. 2000, pp. 77–82.

Simple Deterministic Solutions for Cables Over a Ground Plane or in an Enclosure

Richard H. St. John and Richard Holland

***Abstract*—The use of statistical electromagnetics to determine cable currents in an enclosure consists of two basic parts: 1) determination of the probability density function (pdf) for the ambient electromagnetic fields and 2) substitution of this field pdf in cable-coupling formulas to evaluate the pdf for the cable currents. The application of the work reported here pertains to the second of these operations. Previously, determination of cable-current pdfs was a fairly tedious process involving the solution of finite-difference-like transmission-line equations. Unlike the field-distribution pdfs, the cable-current pdfs could not be expressed, or even approximated, in closed form. The contribution reported here relates the unknown cable-current pdfs to the known field pdfs in closed form and does not require the manipulation of finite-difference entities. Additionally, it turns out that some rather arcane issues concerning the autocorrelation of the electromagnetic cable-driving fields as functions of position or frequency no longer seem to matter.**

***Index Terms*—Cable coupling, cable currents, frequency-domain finite differencing (FDFD), reverberation chambers, statistical electromagnetics (STEM), transmission lines.**

I. Introduction and Equation Presentation

There are two kinds of response in the general case for the current response of a cable in the presence of electromagnetic interference. First, there is the propagating part, which roughly corresponds to the homogeneous portion of the solution of the wave equation on the cable. Next, there is the nonpropagating solution, which represents the driven, or particular, part of the cable current. Much to our surprise, we have recently observed that the homogeneous component is often negligible and may be totally ignored. This approximation appears to work if the cable in question is at least $\lambda/10$ distant from other cables or a ground plane. It may work for even smaller separations, but we have not investigated that case at this time.

For a copper cable of length l, radius a and height h over a ground plane, illuminated by a field E_0 of wavelength λ, terminated at one end by its characteristic impedance (see Fig. 1), $Z_c(a,h,l,\lambda)$ and at the other by $r_{\rm load}$, the propagation-only current on the cable at $r_{\rm load}$ is approximately given by

$$I\left(E_0,a,l,h,r_{\rm load},\lambda\right)=\frac{E_{\rm eff}\left(E_0,h,\lambda\right)\cdot l_{\rm eff}(l,\lambda)}{Z_c(a,h,l,\lambda)+R(a)l_{\rm eff}\left(l,\lambda\right)+r_{\rm load}} \tag{1}$$

where $l_{\rm eff}(l,\lambda)$, the effective cable length, is

$$l_{\rm eff}(l,\lambda)=\frac{1}{\dfrac{1}{l}+\dfrac{1}{\lambda}}=\begin{cases}\lambda, & \text{for } l\gg\lambda\\ l, & \text{for } \lambda\gg l\end{cases} \tag{2}$$

$E_{\rm eff}(E_0,h,\lambda)$, the effective electric field, is

$$E_{\rm eff}\left(E_0,h,\lambda\right)=\frac{E_0}{1+\dfrac{\lambda}{4\pi h}}=\begin{cases}E_0, & \text{for } 4\pi h\gg\lambda\\ 2\dot{B}_0h, & \text{for } \lambda\gg 4\pi h\end{cases} \tag{3}$$

Manuscript received February 11, 2002; revised May 6, 2002.

The authors are with Mission Research Corporation, Albuquerque, NM 87112 USA.

Digital Object Identifier 10.1109/TEMC.2002.804777

0018-9375/02$17.00 © 2002 IEEE